

Article

The Role of Biopolymers on the Water Retention Capacity of Stabilized Sand

Ahmed M. Al-Mahbashi *  and Abdullah Almajed 

Department of Civil Engineering, College of Engineering, King Saud University, Riyadh 11421, Saudi Arabia; alabduallah@ksu.edu.sa

* Correspondence: aalmahbashi@ksu.edu.sa or ena_almahpashi@hotmail.com

Abstract: The application of biopolymers for sand stabilization has recently gained attention due to their natural composition, which makes them both environmentally friendly and of reasonable cost. Measuring the soil–water retention curve (SWRC) of biopolymers-treated sand is essential for the design, modeling, and interpretation of the unsaturated behavior of these materials. Unsaturated shear strength, unsaturated flow, and associated retention capacity are well addressed and evaluated using SWRC. Therefore, this study examined the possible effects of biopolymers—sodium alginate (SA), guar gum (GG), and pectin (P) on the SWRC and retention capacity for stabilized sand. Apart from natural sand, three different concentrations were investigated for each biopolymer. The SWRCs were measured over the entire practical range of suction using a combination of three techniques: hanging column for low suction measurement, axis translation techniques for moderate suction measurement, and vapor equilibrium technique for high suction measurement. The results indicate significant changes in SWRC, and a new series of micropores was developed, this, in turn, extends the desaturation zone of treated sand from a low suction range (i.e., 30 kPa) to moderate to high suction levels (i.e., 10,000 kPa). The saturated water content (w_s) was slightly reduced, air entry values (AEVs), and residual suction (s_r) significantly increased and multiplied up to 200 and 75 times respectively. The retention capacity increased, exhibiting a dependency between the biopolymer type and suction range. The results are of great significance for both practitioner engineers and researchers in predicting the unsaturated soil functions of treated sand.

Keywords: sand; biopolymer-treatment; soil–water retention curve; soil suction; unsaturated soil; retention capacity



Citation: Al-Mahbashi, A.M.; Almajed, A. The Role of Biopolymers on the Water Retention Capacity of Stabilized Sand. *Sustainability* **2024**, *16*, 8612. <https://doi.org/10.3390/su16198612>

Academic Editor: Antonio Caggiano

Received: 28 August 2024

Revised: 26 September 2024

Accepted: 30 September 2024

Published: 4 October 2024



Copyright: © 2024 by the authors. Licensee MDPI, Basel, Switzerland. This article is an open access article distributed under the terms and conditions of the Creative Commons Attribution (CC BY) license (<https://creativecommons.org/licenses/by/4.0/>).

1. Introduction

Sand is a kind of cohesionless soil that covers wide areas around the world. Without confinement, it may lose its stability and strength under low stress. In this context, the use of biopolymers for sand stabilization has recently received increasing attention, since biopolymers are considered to be environment friendly, meaning that they could minimize the environmental hazards caused by the use of other chemical cementitious additives. Moreover, studies conducted on the stabilization of sand using biopolymers have postulated that this addition can effectively control the behavior of sand with regard to its stability, strength, deformation characteristics, and geotechnical properties [1–9].

For instance, Akbulut and Cabalar [10] reported that the addition of biopolymers to sand resulted in a more than twofold increase in unconfined compression strength and California bearing ratio (CBR). Lemboye et al. [11] found that biopolymers significantly improved sand erosion and penetration resistance by 2%, while also enhancing sand stability during drying and wetting cycles by 3% and 5% of the dry weight content. In a practical sense, mixing biopolymers with soil has several potential benefits. Biopolymers—polymers derived from natural sources, such as plants or bacteria can improve the structure and fertility of soil and enhance water retention and nutrient availability [12,13]. Along

these lines, Tran et al. [14] proposed that xanthan gum content can control the loss rate of water from soil under desaturation conditions. Furthermore, Sharma et al. [15] reported that the addition of biopolymers to sandy soil improves the holding capacity of water, meaning that they can be used in arid and semi-arid zones to save irrigation water. Further in-depth investigation about the effect of wetting-drying on the mechanical performance of biopolymer-treated soils and the stability of designed slopes have been addressed in the literature [16,17].

In addition to the mechanical behavior of stabilized sand, its hydromechanical behavior is integral to several geotechnical applications. In such cases, unsaturated soil mechanics are necessary to interpret and understand the unsaturated behavior of these materials (biopolymers-treated sand) Zhang and Liu [18]. The soil-water retention curve (SWRC) depicts the relationship between water content and soil suction—a property that plays a key role in the design and modeling of several geotechnical problems related to shear strength, flow, and volume changes [19–22]. With the availability of SWRCs serving to reduce the time and cost involved in conducting direct measurements of unsaturated shear strength, prediction models for unsaturated shear strength have been widely adopted (i.e., [23–25]) and implemented (i.e., [26–28]) in the literature, with the findings proposing economic and safe design by considering the contribution of suction to shear strength. Furthermore, unsaturated permeability is a crucial property in unsaturated soil mechanics that helps in understanding the flow of water and other types of leaches through soil layers. This property can also be predicted using SWRCs instead of conducting direct measurements [29,30].

Most previous studies conducted on sand treated with different biopolymers have focused on mechanical properties, such as compressive shear strength and penetration tests. More specifically, in the field of study pertaining to saturated soil, Lemboye et al. [11] evaluated the effect of sodium alginate and guar gum biopolymers on the permeability of silica sand by considering different concentrations of biopolymers up to 1%. The results showed a significant reduction in the coefficient of permeability by around half, with the formation of a viscous gel due to the availability of water playing an important role in this reduction. However, studies conducted on unsaturated or hydromechanical sand stabilized using biopolymers remain limited.

In this context, Tran et al. [14] estimated SWRCs for sand treated with different concentrations of xanthan gum biopolymer by performing tests using a pressure plate extractor with suction levels limited to 500 kPa. The results identified an increase in both saturated water content and retention capacity for the treated mixtures, while loss of water during desaturation decreased upon increasing the concentration of biopolymer. Furthermore, Chang and Cho [31] reported that the addition of biopolymer reduces voids between soil particles and enhances the retention capacity of treated sand. Tran et al. [14] found that xanthan gum contributes to the formation of a less steeply sloping SWRC for treated soils. The research conducted by Zhang et al. [18] shed light on the enhancement of Xanthan gum and Gellan gum to the micromechanism of water retention for treated sandy soil, the results indicate an alteration in soil pores and improvement of retention capacity. In other words, xanthan gum content can control the loss rate of water from soil under desaturation conditions, this is also being conducted by Chang et al. [32]. In this context, it is worth noting that most previous studies conducted on SWRCs for sand treated with biopolymers limited themselves to a certain level of suction. In contrast, the current study investigates the SWRC and retention capacity of local sand treated with different biopolymers—sodium alginate (SA), guar gum (GG), and pectin (P) by considering three different concentrations for each polymer type. Furthermore, this study covers the entire range of suction over the different stages; saturation, transition, and up to the residual state by involving three measurement techniques to measure the entire range of soil suction. This is helpful for the construction of SWRC over the entire range of suction, and this relation becomes a key tool for modeling and predicting the unsaturated soil behavior for liner materials. In addition, the possible effects of retention capacity and the main characteristics

of SWRC at different stages are discussed, highlighted, and supported by scanning electron microscope images.

2. Materials Used

The materials examined in this study are local sands available in the vicinity of Riyadh city, specifically in the Althumamah area. According to geotechnical investigations conducted in the laboratory, the specific gravity of this sand was 2.68 as per ASTM D854 [33]. The results of a grain size analysis conducted on a dry sample of the sample sand based on ASTM D6913 [34] are shown in Figure 1. Furthermore, an examination of the gradation curve based on ASTM D2487 [35] revealed a poorly graded curve of fine sand. The values of D₁₀, D₃₀, and D₆₀ were 0.143, 0.182, and 0.245, respectively. These values yielded a coefficient of concavity (Cc) of 0.95 and a uniformity coefficient (Cu) of 1.71. A compaction test conducted following ASTM D698 [36] for the material revealed a maximum dry density of 1.65 and an optimum moisture content of 11%.

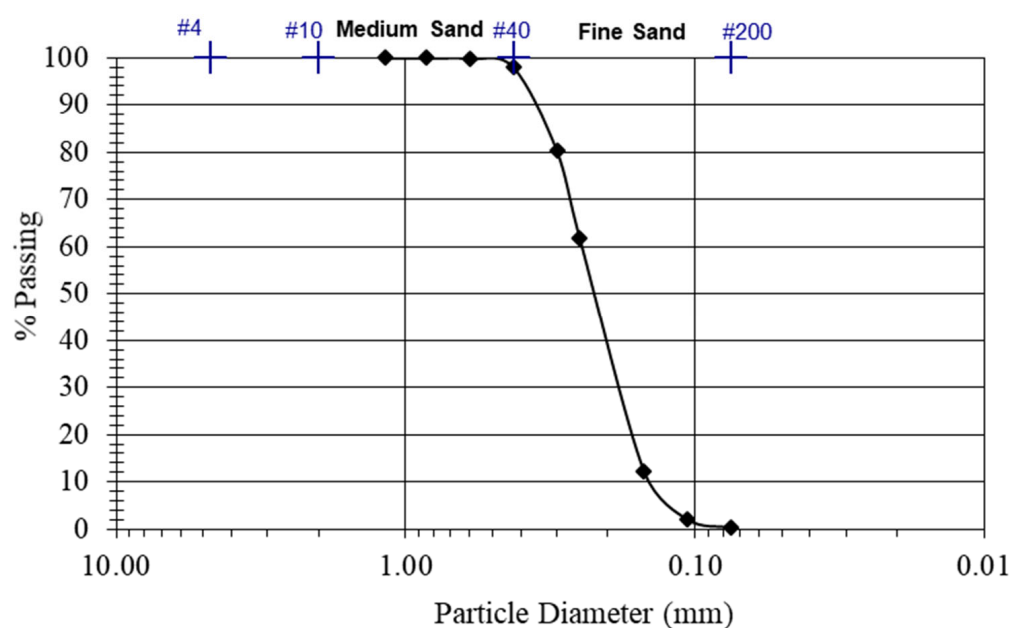


Figure 1. Gradation curve of the sand used in this study.

The biopolymers examined in this investigation were sodium alginate (SA), pectin (P), and guar gum (GG). Most of the previous studies in the literature were conducted on the Xanthan biopolymers, in the study the other types were selected based on sustainability, availability, thickening and film formation, gelling capability, and simplicity of use. Furthermore, these biopolymers were proven to have a significant effect regarding stability and shear strength for the same treated materials of sand [37].

Sodium alginate is a linear polysaccharide derived from alginic acid that consists of α -L-guluronic (G) and 1,4- β -D-mannuronic (M) acids. Notably, sodium alginate—a component found in the cell walls of marine brown algae—contains between 30% and 60% alginic acid. Pectin is a macromolecule composed of several distinct polysaccharides that can be extracted from plants. Guar gum is a natural thickening agent derived from guar beans.

3. Experimental Work

In this section, the testing variables used were defined initially. The mixtures and specimen preparation were presented in this section followed by the determination of SWRC.

3.1. Testing Variables

In this study, three different biopolymers were considered including sodium alginate (SA), pectin (P), and guar gum (GG). Different concentrations of biopolymers—1%, 3%,

and 5% for sodium alginate, pectin, and guar gum, were considered for each type. These concentrations were selected based on previous studies conducted on the same materials [37]. Moreover, these values are also within the practical range proposed by several studies [38,39]. Notably, Lemboye and Almajed [37] reported significant improvement in the unconfined compressive strength of sand modified using pectin and sodium alginate, with the values doubling several times to reach a maximum of 600 kPa. The soil suction measurement was conducted over the entire range of suction using a combination of hanging column, axis translation, and vapor equilibrium techniques.

3.2. Mixtures and Specimen Preparation

In this study, the wet-mixing technique was implemented to prepare the different concentrations of biopolymers—1%, 3%, and 5% for sodium alginate, pectin, and guar gum, respectively. The wet-mixing technique offers the advantage of creating a homogenous mixture that allows the solution to access and cover more particle surfaces [40]. The biopolymers were added to distilled water in small quantities and then mixed thoroughly using a mechanical mixer. This step may extend to 30 min until a homogeneous mixture is attained. Subsequently, the water content corresponding to the optimum moisture content was added to the dry sand and mixed until a homogeneous mixture was achieved. A reference mixture of pure sand was also prepared by mixing dry sand with the optimum moisture content.

The specimens were compacted into suitable rings (i.e., 50–80 mm in diameter and 20 mm in height) to achieve the maximum dry density predetermined by the compaction curve. The compacted specimens were then kept in an isolated room for a curing period of 7 days, with the temperature in the surrounding environment being around 23 ± 1 °C. Following this, the specimens were mounted on the oedometer cell, after which inundation with distilled water was performed to ensure the saturation condition of the specimens before commencing the determination of SWRCs.

3.3. Soil Water Retention Curve Determination

The SWRCs were determined using three different techniques hanging column, axis translation technique, and vapor equilibrium technique to account for the entire range of suction since each technique has a specific limit for suction measuring (limited range of suction). Notably, standard test methods for determining the soil water characteristic curve for desorption using these techniques are described in ASTM D6836 [41].

The hanging column technique is generally utilized to measure the low suction range (less than 10 kPa) of granular materials, such as sandy soils [41]. This technique involves a water outflow graduated burette, a suction application burette, and a glass Buchner funnel with a porous plate, as illustrated in Figure 2a. The compacted specimen is placed in good contact above the porous plate to obtain saturation and equilibration at zero suction level. Next, the test specimen is subjected to matric suction by increasing the difference between the specimen's elevation and the water level's elevation in the suction application burette. The device maintains a suction control resolution of 0.01 kPa, and the elevation difference can be adjusted at a resolution of 1 mm. At equilibrium, the suction value can be computed by multiplying the variation in the water levels with the unit weight of water. The water content corresponding to the suction value can then be computed from the outflow of water or by using the gravimetric method.

The axis translation technique can impose a matric suction of up to 1500 kPa, with the level of suction governed by the high air-entry value ceramic disk used to separate the air and water phases [41]. The device widely used for this purpose is a pressure plate extractor, which provides reliable suction measurements, i.e., [42–44]. In addition to the high air-entry value (HAEV) ceramic disk, the pressure plate extractor comprises a pressure cell and a control panel, as shown in Figure 2b. An outer source of compressed air is used to apply air pressure on the soil specimens placed above the saturated HAEV disk. The saturated HAEV disk plays a main role in separating water and air phases during suction

measurement. In this study, several increments of matric suction were sequentially applied (10, 20, 50, 100, 200, up to 1400 kPa). Each increment was maintained until the equilibrium state was reached (the state at which no further discharge of water from the specimens was recorded). The weight of the specimen and its final dimensions were recorded, and the water content after each suction increment was calculated.

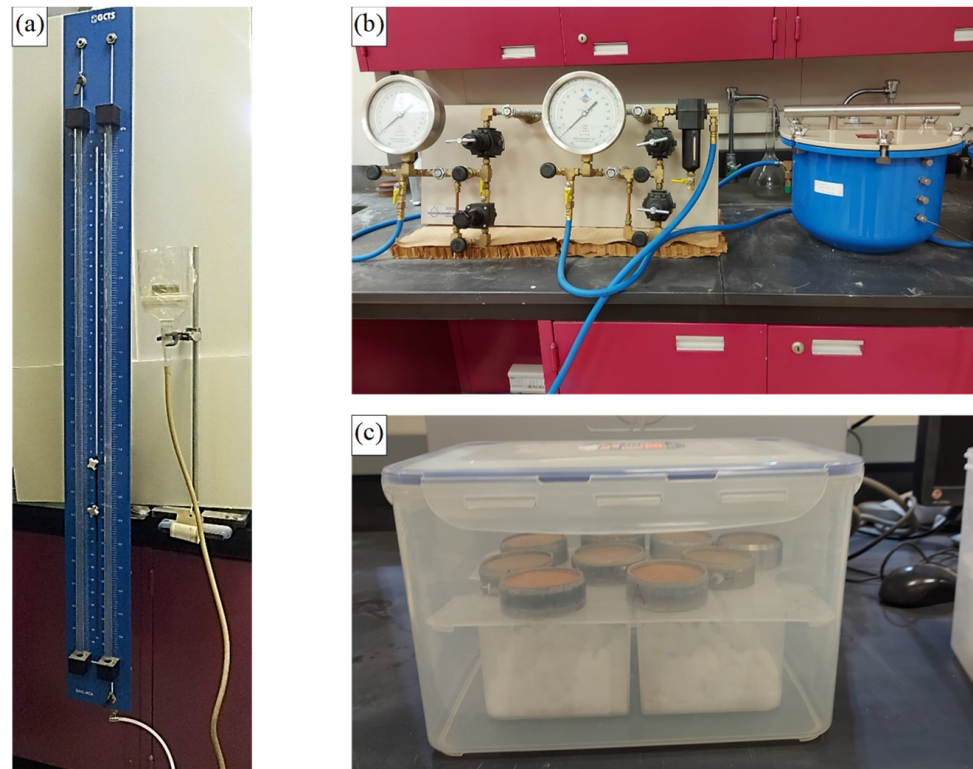


Figure 2. Testing devices for the considered techniques: (a) hanging column, (b) pressure plate extractor, and (c) saturated salt solutions.

The vapor equilibrium technique was performed using different saturated salt solutions to obtain measurements pertaining to a high suction range of more than 1500 kPa. In this technique, suction is imposed by placing the soil specimen in an isolated box with constant relative humidity. When the specimen achieves equilibrium, the relationship between the relative humidity and suction can be computed using the Kelvin equation [19], which is as follows:

$$\psi = \frac{RT\rho_w}{w} \ln \left[\frac{1}{RH} \right] \quad (1)$$

where, ψ = soil suction (kPa), R = molar gas constant (8.314462 J/(mol K)), T = absolute temperature (K), w = molecular mass of water vapor (18.016 g/mol), ρ_w = is the mass density of water (kg/m³), and RH = relative humidity.

In this study, the appropriate amount of saturated salt solution was prepared according to ASTM E 104 [45] based on the known RH , after which it was placed in an isolated box. The soil specimens were suspended over the salt solution to attain equilibrium under the given RH , as shown in Figure 2c. The weights of the specimens were measured and recorded periodically. When subsequent records of the weights were equal or close to each other, it was assumed that an equilibrium state had been reached. Figure 3 presents the results of the equilibrium process for the specimens treated with different salt solutions. It is evident that the specimens showed different rates of moisture loss, with those treated with guar gum biopolymer undergoing higher moisture loss during equilibration. The water content and specimen dimensions corresponding to the imposed suctions were also obtained.

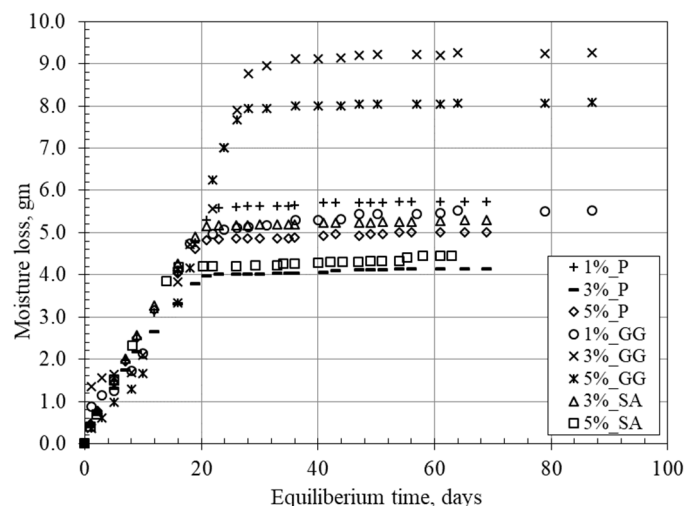


Figure 3. Equilibrium process under different salt solutions, using the vapor equilibrium technique.

4. Results and Discussion

The following section demonstrates the results achieved by the experiments conducted in this investigation. The tests were conducted considering several points of measurement even at low suctions to be close to each other, at this level the measured points were clearly depicted in figures and a simple line between measured points was initiated with any fitting models after which the effects of biopolymer type and biopolymer content on SWRC and retention characteristics are discussed.

4.1. Effect of Biopolymer Content on SWRCs

This section discusses the possible effects of the selected biopolymers on the SWRCs of the treated sand. Figure 4a–c present the SWRCs, in terms of water content versus suction, of the sand treated with different concentrations of sodium alginate (SA), pectin (P), and guar gum (GG), respectively. The SWRC for the natural sand used in this study before treatment is included as a reference in all figures. Regardless of the type of biopolymer, dramatic changes were noticed in the SWRCs, marked by a notable reduction in saturated water content due to the addition of biopolymers, which resulted in the occupation of the large pores by biopolymer components.

The profile of SWRCs over the entire range of suction can be physically identified as having three main zones the saturated or boundary effect zone, the transition or desaturation zone, and the residual zone, i.e., [46,47] as depicted in Figure 5. The SWRC clearly related to the pore size distribution of soil, and these zones are defined based on the flow of water in the different series of distributed pore sizes [48,49]. Three main parameters are identified the boundary of these zones namely, saturated water content (w_s), air entry value (AEV), and residual water content (w_r). The shape of SWRC could be varied to a bimodal curve with two distinguished air entry values (AEV₁ and AEV₂) for soil with dual pore size series, more information regarding the unimodal and bimodal shapes of SWRC are provided in literature [50,51]. The zones of SWRC are characterized by the amount of water in the soil pores and pore size distribution, which are controlled by the two mechanisms of capillary and adsorption [47,52,53]. The identified zones of SWRC are shown in Figure 5. The saturated zone is the zone where large pores are mostly filled with free water. This zone is governed by a capillary mechanism and can extend up to the air-entry value (AEV). At this suction value (i.e., AEV), water starts to exit the large pores, and this desaturation of the soil continues until it reaches a residual state. This zone is identified as the desaturation or transition zone. The last zone is the residual zone, characterized by a stable volume, water film strongly attracted to the particle surface, and no further change in volume due to further desaturation.

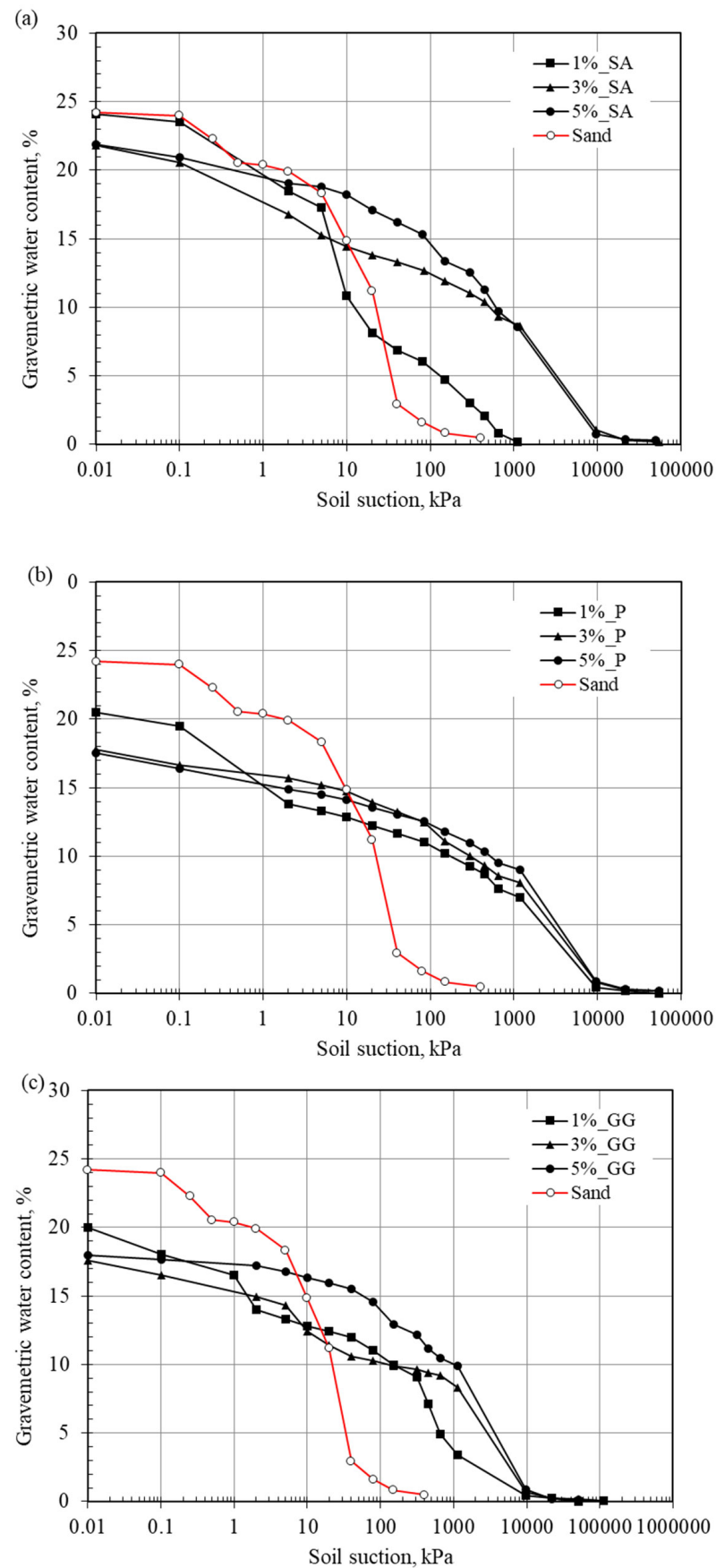


Figure 4. Effect of biopolymer percentage on SWRCs: (a) sodium alginate, (b) pectin, and (c) guar gum.

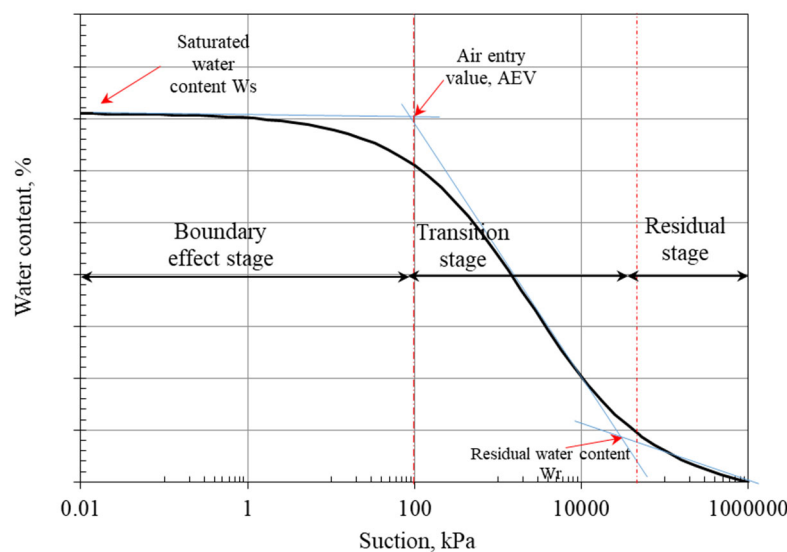


Figure 5. A typical SWRC with its identified zones.

In the saturation zone (i.e., free water), the effect of the tested polymers on retention capacity seemed to have only a slight effect on the SWRCs, with a reduction of w_s occurring due to the occupation of the large pores by the polymer component. The plausible effect of polymers on SWRCs started appearing in the desaturation zone, where their retention capacity was observed to be significantly enhanced. This is attributed to the nature of biopolymer powder and the produced gel component which mostly affects the micropores and as mentioned before the desaturation zone is mainly governed by the micropores [54,55]. As shown in Figure 5, the untreated or natural sand was desaturated within the low suction range of up to 30 kPa, while the desaturation zone for the treated ones enlarged up to a high level of suction (i.e., 10,000 kPa). Notably, it was observed that the profile of the SWRC enlarged to cover the entire range of suction. Furthermore, while the residual state of pure sand was estimated at a suction value of 100 kPa, the treated specimens achieved an estimated residual state at around 10,000 kPa, which has been doubled ten times. This enhancement in retention capacity can be attributed to the gel component produced from biopolymers dissolving in water. The scanning electron microscope images of the natural sand and the treated specimens are presented in Figure 6a–c. An analysis of these images revealed that the gel component filled the macropores of sand and surrounded the particles (Figure 6b).

The gel-like nature of biopolymers in aqueous solutions represents its greatest benefit. A low-viscosity solution quickly attains a gel structure when monovalent ions, such as sodium in sodium alginate, are swapped for divalent ions, particularly calcium. The new constellation of particles produces a new series of smaller micropores (Figure 6b–d), which contribute to producing a wide transition zone reaching 10,000 kPa of suction.

4.2. Effect of Biopolymer Type on Retention Capacity

Figure 7a–c present the effects of biopolymer types on the retention capacity of the treated sand at dosages of 1%, 3%, and 5%, respectively. At a low dosage of polymers (Figure 7a), SA exhibited a higher retention capacity at the low suction level (less than 10 kPa). However, beyond this value of suction (i.e., 10 kPa), the specimen treated with SA was desaturated at a faster rate, while the P and GG specimens exhibited a higher retention capacity. On increasing the polymer content to 3%, SA continued to display higher retention capacity at both the low range and high range of suction. Finally, at the highest dosage of polymers, SA induced a higher retention capacity. As shown in Figure 6b,c, the flaky shape of the developed gel component induced micropore formation, which enhanced the retention capacity under SA more than under P, as shown in Figure 6d. In this regard, it is worth noting that the effect of biopolymers tends to be paramount at high suction

levels because, in this zone (i.e., the residual zone), water remains tightly bound to the microstructure pores due to adsorption.

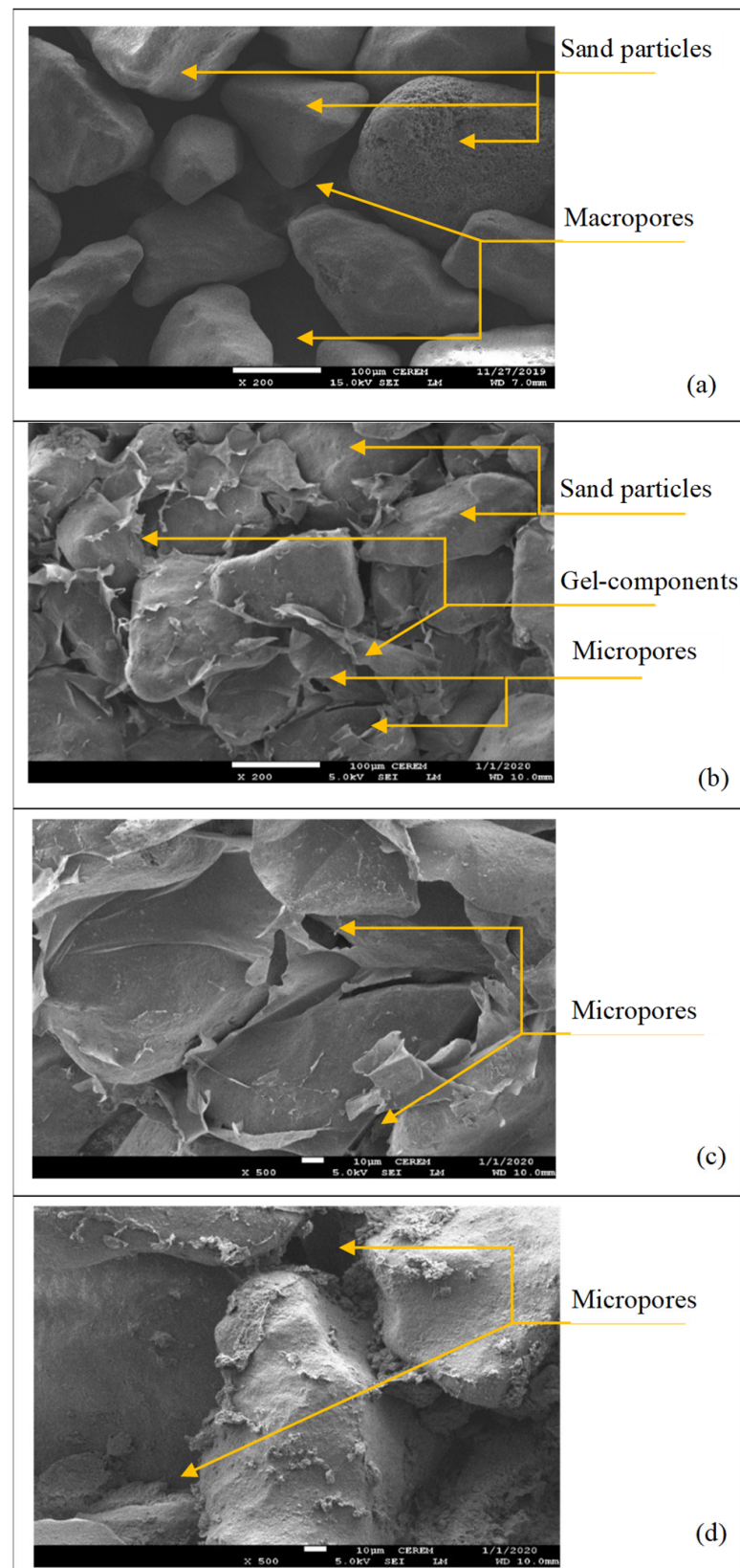


Figure 6. SEM images of (a) natural sand, (b,c) specimens treated with SA, and (d) specimens treated with P.

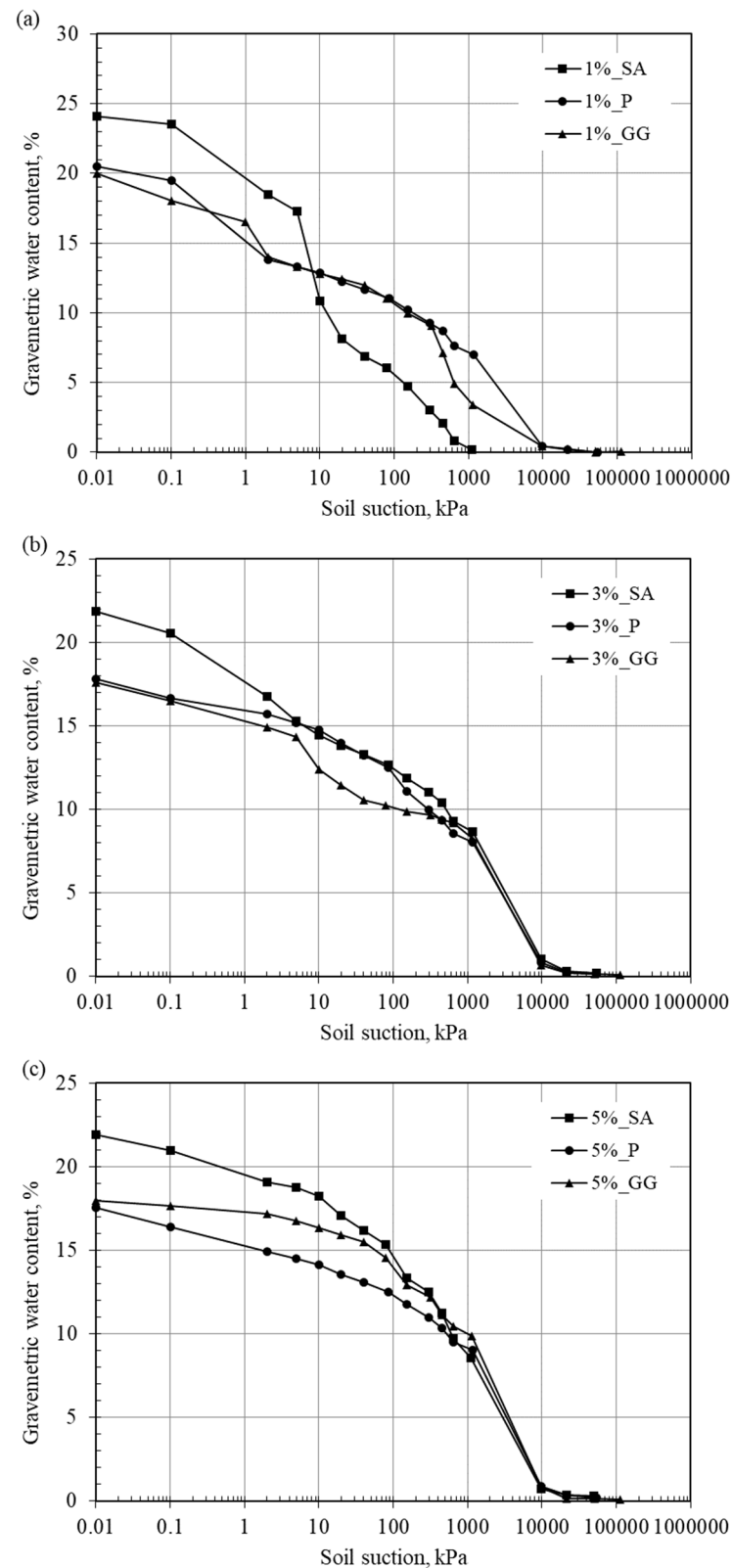


Figure 7. Effect of biopolymer type on SWRCs of sand at different biopolymer dosages: (a) 1%, (b) 3%, and (c) 5%.

Variations in the main characteristics of SWRCs with regard to different biopolymer types and contents are summarized in Figure 8. These parameters may play an important role in the interpretation, modeling, and design of unsaturated soil behavior in geotech-

nical and geoenvironmental applications. As depicted in Figure 8a, the saturated water content (w_s) showed a decreasing trend with increasing biopolymer content, with the entire reduction being about 9% for SA and 27% for P and GG. As mentioned earlier, this occurs because the gel components occupy the sand pores, thus affecting the saturation capacity. Furthermore, AEV1 and AEV2 increased several times with increasing biopolymer content, as shown in Figure 8b–d indicates that both residual suction and residual water content increased due to the extension in the residual zone achieved by the biopolymers.

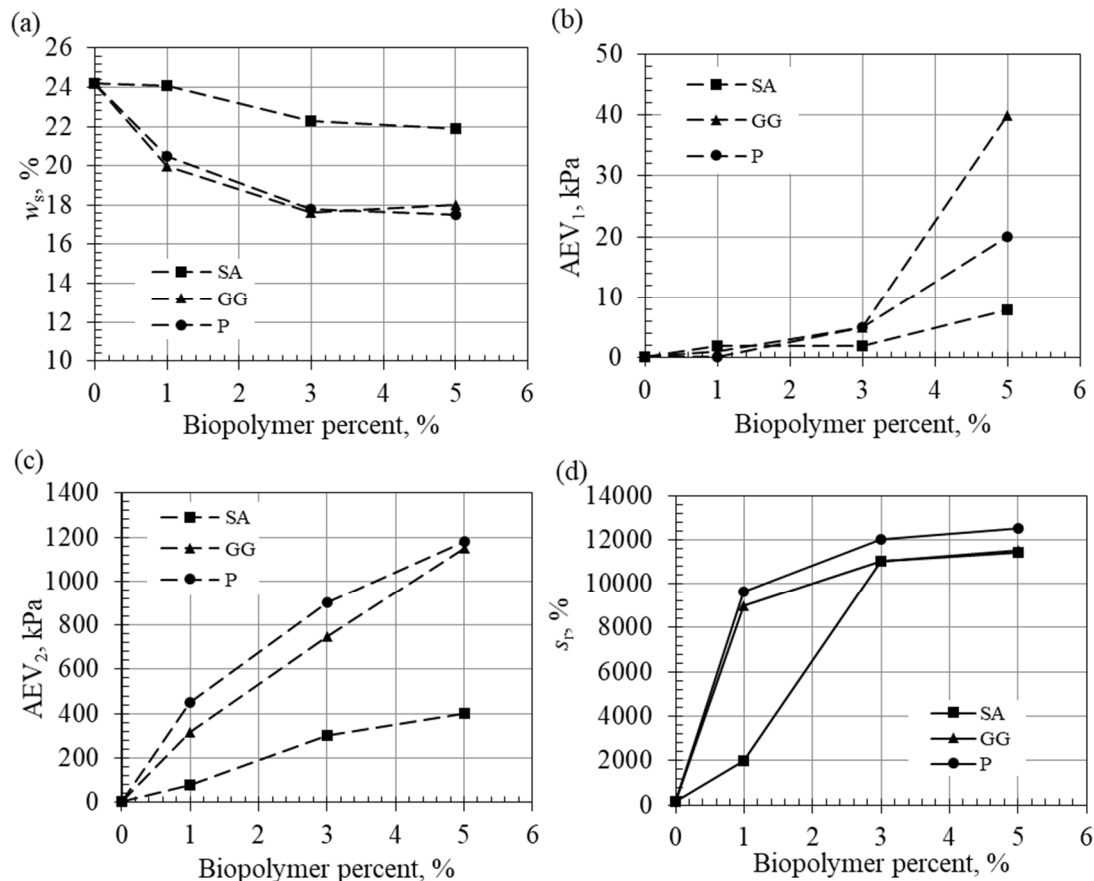


Figure 8. Changes induced by biopolymers in the main characteristics of SWRCs: (a) w_s , (b) AEV1, (c) AEV2, and (d) s_r .

5. Conclusions

The main findings of this study can be summarized as follows:

- Biopolymers induced significant changes in the different stages of SWRCs of the treated samples. In the saturation zone, biopolymers only had a slight effect on the retention capacity of the treated sand, with the saturated water content (w_s) reducing by 9% for the SA specimen and 26% for the P and GG specimens.
- The plausible effect of biopolymers was observed in the desaturation zone, the untreated sand was desaturated within a low suction level range of up to 30 kPa, and the desaturation zone of the treated specimen enlarged up to a high level of suction (i.e., 10,000 kPa). Furthermore, the AEV_{1,2} of the treated specimens doubled several times.
- While the residual stage of pure sand was limited to the suction level of 30 kPa, the residual stage of the treated specimens reached was doubled tenths times and reached a 10,000 kPa of suction, which doubled ten times.
- The enhancement of the retention capacity can be attributed to the gel component produced from biopolymers dissolving in water, as detected from the scanning electron

microscope images. This component filled the voids surrounding the sand particles and created a new series of micropores.

- At the highest content of biopolymer, SA exhibited the highest retention capacity up to a moderate level of suction. In this context, it is worth noting that the effect of biopolymers tends to be paramount at high suction levels (more than 1000 kPa).

The obtained results in this study are of great significance to help practitioners and engineers on conducting a safe and sustainable design using the advancement of unsaturated soil mechanics. Further future works are recommended regarding the unsaturated behavior of biopolymer-treated sand including unsaturated flow and unsaturated shear strength.

Author Contributions: Conceptualization, A.M.A.-M. and A.A.; methodology, A.M.A.-M. and A.A.; software, A.M.A.-M.; validation, A.M.A.-M.; formal analysis, A.M.A.-M.; investigation, A.M.A.-M.; resources, A.M.A.-M. and A.A.; data curation, A.M.A.-M.; writing—original draft preparation, A.M.A.-M.; writing—review and editing, A.M.A.-M. and A.A.; visualization, A.M.A.-M.; supervision, A.A.; project administration, A.M.A.-M. and A.A.; funding acquisition, A.A. All authors have read and agreed to the published version of the manuscript.

Funding: This research is funded by the Researchers Supporting Project number (RSP2024R279), King Saud University, Riyadh, Saudi Arabia.

Institutional Review Board Statement: Not applicable.

Informed Consent Statement: Not applicable.

Data Availability Statement: The data used to support the findings of this study are included in the figures shown.

Acknowledgments: The authors would like to acknowledge the Researchers Supporting Project number (RSP2024R279), King Saud University, Riyadh, Saudi Arabia.

Conflicts of Interest: The authors declare that they have no conflict of interest.

References

1. Chang, I.; Im, J.; Cho, G.C. Geotechnical engineering behaviors of gellan gum biopolymer treated sand. *Can. Geotech. J.* **2016**, *53*, 1658–1670. [\[CrossRef\]](#)
2. Chang, I.; Im, J.; Prasidhi, A.K.; Cho, G.C. Effects of Xanthan gum biopolymer on soil strengthening. *Constr. Build. Mater.* **2015**, *74*, 65–72. [\[CrossRef\]](#)
3. Lee, S.; Chung, M.; Park, H.M.; Song, K.I.; Chang, I. Xanthan gum biopolymer as soil-stabilization binder for road construction using local soil in Sri Lanka. *J. Mater. Civ. Eng.* **2019**, *31*, 06019012. [\[CrossRef\]](#)
4. Almajed, A.; Lemboye, K.; Arab, M.G.; Alnuaim, A. Mitigating wind erosion of sand using biopolymer-assisted EICP technique. *Soils Found.* **2020**, *60*, 356–371. [\[CrossRef\]](#)
5. Ni, J.; Hao, G.L.; Chen, J.Q.; Ma, L.; Geng, X.Y. The optimisation analysis of sand-clay mixtures stabilised with xanthan gum biopolymers. *Sustainability* **2021**, *13*, 3732. [\[CrossRef\]](#)
6. Prakash, S.S.J.; Naidu, M.Y. Performance Evaluation of Polysachharide based Biomaterials for Sand Stabilization. *Int. J. Sci. Res. Eng. Manag.* **2023**, *7*, 1–13. [\[CrossRef\]](#)
7. Fortuna, B.; Logar, J.; Sorze, A.; Valentini, F.; Smolar, J. Influence of Xanthan Gum-Based Soil Conditioners on the Geotechnical Properties of Soils. *Appl. Sci.* **2024**, *14*, 4044. [\[CrossRef\]](#)
8. Zhang, J.; Liu, J. A Review on Soils Treated with Biopolymers Based on Unsaturated Soil Theory. *Polymers* **2023**, *15*, 4431. [\[CrossRef\]](#)
9. Ni, J.; Li, S.S.; Ma, L.; Geng, X.Y. Performance of soils enhanced with eco-friendly biopolymers in unconfined compression strength tests and fatigue loading tests. *Constr. Build. Mater.* **2020**, *263*, 120039. [\[CrossRef\]](#)
10. Akbulut, N.; Cabalar, A.F. Effects of biopolymer on some geotechnical properties of a sand. In *New Frontiers in Geotechnical Engineering*; ASCE: Reston, VA, USA, 2014; pp. 28–37.
11. Lemboye, K.; Almajed, A.; Hamid, W.; Arab, M. Permeability investigation on sand treated using enzyme-induced carbonate precipitation and biopolymers. *Innov. Infrastruct. Solut.* **2021**, *6*, 167. [\[CrossRef\]](#)
12. Wang, S.; Zhao, X.; Zhang, J.; Jiang, T.; Wang, S.; Zhao, J.; Meng, Z. Water retention characteristics and vegetation growth of biopolymer-treated silt soils. *Soil Tillage Res.* **2023**, *225*, 105544. [\[CrossRef\]](#)
13. Ni, J.; Wang, Z.T.; Geng, X.Y. Vegetation growth promotion and overall strength improvement using biopolymers in vegetated soils. *Can. Geotech. J.* **2023**, *61*, 1294–1310. [\[CrossRef\]](#)
14. Tran, T.P.A.; Cho, G.C.; Ilhan, C. Water Retention Characteristics of Biopolymer Hydrogel-Treated Sand-Clay Mixture. *Earth Sci. Environ.* **2020**, *127*, 5–17. [\[CrossRef\]](#)

15. Sharma, R.; Bajpai, J.; Bajpai, A.K.; Acharya, S.; Kumar, B.; Singh, R.K. Assessment of water retention performance of pectin-based nanocarriers for controlled irrigation in agriculture. *Agric. Res.* **2017**, *6*, 139–149. [\[CrossRef\]](#)
16. Chen, Z.; Liu, J.; Wang, Y.; Qi, C.; Ma, X.; Che, W.; Ma, K. Wetting–drying effects on the mechanical performance of xanthan gum biopolymer-stabilized soil. *Environ. Earth Sci.* **2024**, *83*, 197. [\[CrossRef\]](#)
17. Seo, S.; Lee, M.; Im, J.; Kwon, Y.M.; Chung, M.K.; Cho, G.C.; Chang, I. Site application of biopolymer-based soil treatment (BPST) for slope surface protection: In-situ wet-spraying method and strengthening effect verification. *Constr. Build. Mater.* **2021**, *307*, 124983. [\[CrossRef\]](#)
18. Zhang, J.; Liu, J.; Cheng, Y.; Jiang, T.; Saberian, M. Water-retention behaviour and microscopic analysis of two biopolymer-improved sandy soils. *Constr. Build. Mater.* **2023**, *403*, 133202. [\[CrossRef\]](#)
19. Fredlund, D.G.; Rahardjo, H. *Soil Mechanics for Unsaturated Soils*; Wiley InterScience: New York, NY, USA, 1993.
20. Fredlund, D.G. The 1999 R.M. Hardy lecture: The implementation of unsaturated soil mechanics into geotechnical engineering. *Can. Geotech. J.* **2000**, *37*, 963–986. [\[CrossRef\]](#)
21. Al-Mahbashi, A.M.; Elkady, T.Y.; Alrefeai, T.O. Soil water characteristic curve and improvement in lime treated expansive soil. *Geomech. Eng.* **2015**, *8*, 687–706. [\[CrossRef\]](#)
22. Bozyigit, I.; Javadi, A.; Altun, S. Strength properties of xanthan gum and guar gum treated kaolin at different water contents. *J. Rock Mech. Geotech. Eng.* **2021**, *13*, 1160–1172. [\[CrossRef\]](#)
23. Lee, S.J.; Lee, S.R.; Kim, Y.S. An approach to estimate unsaturated shear strength using artificial neural network and hyperbolic formulation. *Comput. Geotech.* **2003**, *30*, 489–503. [\[CrossRef\]](#)
24. Garven, E.A.; Vanapalli, S.K. Evaluation of empirical procedures for predicting the shear strength of unsaturated soils. In Proceedings of the Unsaturated Soils 2006, Carefree, AZ, USA, 2–6 April 2006; pp. 2570–2592.
25. Lee, I.M.; Sung, S.G.; Cho, G.C. Effect of stress state on the unsaturated shear strength of a weathered granite. *Can. Geotech. J.* **2005**, *42*, 624–631. [\[CrossRef\]](#)
26. Fredlund, D.G.; Vanapalli, S.K.; Pufahl, D.E. Predicting the shear strength function for unsaturated soils using the soil-water characteristic curve. In Proceedings of the First International Conference on Unsaturated Soils/Unsat'95, Paris, France, 6–8 September 1995; Volume 1.
27. Goh, S.G.; Rahardjo, H.; Leong, E.C. Shear strength of unsaturated soils under multiple drying-wetting cycles. *J. Geotech. Geoenviron. Eng.* **2014**, *140*, 06013001. [\[CrossRef\]](#)
28. Al-Mahbashi, A.M.; Elkady, T.Y. Prediction of unsaturated shear strength of expansive clays. *Proc. Inst. Civ. Eng. Geotech. Eng.* **2017**, *170*, 407–420. [\[CrossRef\]](#)
29. Fredlund, D.G.; Xing, A.; Huang, S. Predicting the permeability function for unsaturated soils using the soil-water characteristic curve. *Can. Geotech. J.* **1994**, *31*, 533–546. [\[CrossRef\]](#)
30. Li, J.H.; Zhang, L.M.; Li, X. Soil-water characteristic curve and permeability function for unsaturated cracked soil. *Can. Geotech. J.* **2011**, *48*, 1010–1031. [\[CrossRef\]](#)
31. Chang, I.; Cho, G.C. Shear strength behavior and parameters of microbial gellan gum-treated soils: From sand to clay. *Acta Geotech.* **2019**, *14*, 361–375. [\[CrossRef\]](#)
32. Chang, I.; Cho, G.C.; An Tran, T.P. Water-retention properties of xanthan-gum-biopolymer-treated soils. *Environ. Geotech.* **2023**, *11*, 152–163. [\[CrossRef\]](#)
33. ASTM D854-14; Standard Test Methods for Specific Gravity of Soil Solids by Water Pycnometer. ASTM International: West Conshohocken, PA, USA, 2014.
34. ASTM D6913-09; Standard Test Methods for Particle-Size Distribution (Gradation) of Soils Using Sieve Analysis. ASTM International: West Conshohocken, PA, USA, 2009.
35. ASTM D2487-17; Standard Practice for Classification of Soils for Engineering Purposes (Unified Soil Classification System). ASTM International: West Conshohocken, PA, USA, 2017. [\[CrossRef\]](#)
36. ASTM D698-2018; Standard Test Methods for Laboratory Compaction Characteristics of Soil Using Standard Effort (12,400 ft-lbf/ft³ (600 kNm/m³)). ASTM International: West Conshohocken, PA, USA, 2000.
37. Lemboye, K.; Almajed, A. Effect of varying curing conditions on the strength of biopolymer modified sand. *Polymers* **2023**, *15*, 1678. [\[CrossRef\]](#)
38. Biju, M.S.; Arnepalli, D.N. Effect of biopolymers on permeability of sand-bentonite mixtures. *J. Rock Mech. Geotech. Eng.* **2020**, *12*, 1093–1102. [\[CrossRef\]](#)
39. Ghasemzadeh, H.; Modiri, F.; Darvishan, E. A novel clean biopolymer-based additive to improve mechanical and microstructural properties of clayey soil. *Clean Technol. Environ. Policy* **2022**, *24*, 969–981. [\[CrossRef\]](#)
40. Theng, B.K.G. *Formation and Properties of Clay-Polymer Complexes*; Elsevier: Amsterdam, The Netherlands, 2012.
41. ASTM D6836; Standard Test Methods for Determination of the Soil Water Characteristic Curve for Desorption Using a Hanging Column, Pressure Extractor, Chilled Mirror Hygrometer, and/or Centrifuge. ASTM International: West Conshohocken, PA, USA, 2016.
42. Pham, Q.H.; Fredlund, D.G.; Padilla, J.M. Use of the GCTS apparatus for the measurement of soil-water characteristic curves. In Proceedings of the 57th Canadian Geotechnical Conference, Quebec City, QC, Canada, 24–27 October 2004; pp. 24–27.
43. Padilla, J.M.; Perera, Y.Y.; Houston, W.N.; Fredlund, D.G. A new soil-water characteristic curve device. In Proceedings of the Advanced Experimental Unsaturated Soil Mechanics, an International Symposium, EXPERUS 2005, Trento, Italy, 27–29 June 2005; A.A. Balkema Publishers: Leiden, The Netherlands, 2005; pp. 15–22.

44. Al-Mahbashi, A.M.; Elkady, T.Y.; Al-Shamrani, M.A. Hysteresis soil-water characteristic curves of highly expansive clay. *Eur. J. Environ. Civ. Eng.* **2018**, *22*, 1041–1059. [[CrossRef](#)]
45. ASTM E 104; Standard Practice for Maintaining Constant Relative Humidity by Means of Aqueous Solutions. ASTM International: West Conshohocken, PA, USA, 2007.
46. Fredlund, D.G.; Xing, A.; Fredlund, M.D.; Barbour, S.L. The relationship of the unsaturated soil shear strength to the soil-water characteristic curve. *Can. Geotech. J.* **1996**, *33*, 440–448. [[CrossRef](#)]
47. Lu, N.; Likos, W.J. *Unsaturated Soil Mechanics*; Wiley: New York, NY, USA, 2004.
48. Lu, N. Generalized soil water retention equation for adsorption and capillarity. *J. Geotech. Geoenviron. Eng.* **2016**, *142*, 04016051. [[CrossRef](#)]
49. Luo, S.; Zhou, B.; Likos, W.J.; Lu, N. Determining Capillary Pore-Size Distribution of Soil from Soil-Water Retention Curve. *J. Geotech. Geoenviron. Eng.* **2024**, *150*, 04023138. [[CrossRef](#)]
50. Satyanaga, A.; Rahardjo, H.; Leong, E.C.; Wang, J.Y. Water characteristic curve of soil with bimodal grain-size distribution. *Comput. Geotech.* **2013**, *48*, 51–61. [[CrossRef](#)]
51. Al-Mahbashi, A.M.; Dafalla, M.; Al-Shamrani, M. Predicting soil-water characteristic curves of expansive soils relying on correlations. *Geomech. Eng.* **2023**, *33*, 625–633.
52. Tuller, M.; Or, D.; Dudley, L.M. Adsorption and capillary condensation in porous media: Liquid retention and interfacial configurations in angular pores. *Water Resour. Res.* **1999**, *35*, 1949–1964. [[CrossRef](#)]
53. Lu, N.; Khorshidi, M. Mechanisms for soil-water retention and hysteresis at high suction range. *J. Geotech. Geoenviron. Eng.* **2015**, *141*, 04015032. [[CrossRef](#)]
54. Nassiri, S.; Zapata, C.; Mahabadi, N. Evolution of Water Retention Characteristics in Bio-Geochemically Altered Unsaturated Soils: A Pore-Scale Study. *E3S Web Conf.* **2023**, *382*, 18004. [[CrossRef](#)]
55. Chen, H.; Feng, S.J. A simple water retention model of dual-porosity soils based on self-similarity of bimodal pore size distribution. *Comput. Geotech.* **2023**, *162*, 105684. [[CrossRef](#)]

Disclaimer/Publisher’s Note: The statements, opinions and data contained in all publications are solely those of the individual author(s) and contributor(s) and not of MDPI and/or the editor(s). MDPI and/or the editor(s) disclaim responsibility for any injury to people or property resulting from any ideas, methods, instructions or products referred to in the content.